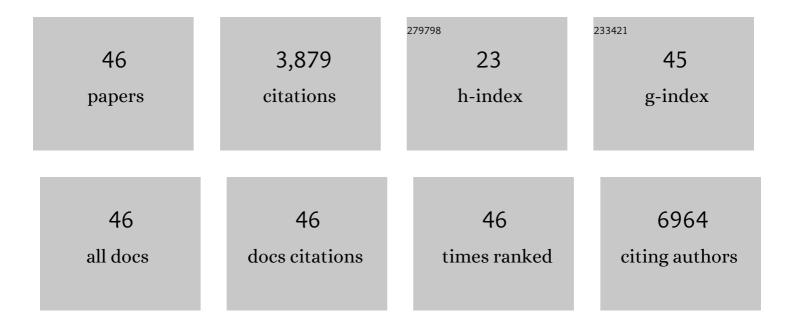
## Yifan Ye

## List of Publications by Year in descending order

Source: https://exaly.com/author-pdf/10382031/publications.pdf Version: 2024-02-01



#	Article	IF	CITATIONS
1	High-Rate, Ultralong Cycle-Life Lithium/Sulfur Batteries Enabled by Nitrogen-Doped Graphene. Nano Letters, 2014, 14, 4821-4827.	9.1	683
2	Coordinatively unsaturated nickel–nitrogen sites towards selective and high-rate CO <sub>2</sub> electroreduction. Energy and Environmental Science, 2018, 11, 1204-1210.	30.8	622
3	Enabling unassisted solar water splitting by iron oxide and silicon. Nature Communications, 2015, 6, 7447.	12.8	429
4	Stable iridium dinuclear heterogeneous catalysts supported on metal-oxide substrate for solar water oxidation. Proceedings of the National Academy of Sciences of the United States of America, 2018, 115, 2902-2907.	7.1	229
5	<i>Acacia Senegal</i> –Inspired Bifunctional Binder for Longevity of Lithium–Sulfur Batteries. Advanced Energy Materials, 2015, 5, 1500878.	19.5	223
6	Oxygen evolution reaction over catalytic single-site Co in a well-defined brookite TiO2 nanorod surface. Nature Catalysis, 2021, 4, 36-45.	34.4	189
7	Oxidation State and Surface Reconstruction of Cu under CO <sub>2</sub> Reduction Conditions from <i>In Situ</i> X-ray Characterization. Journal of the American Chemical Society, 2021, 143, 588-592.	13.7	172
8	Safe and Durable High-Temperature Lithium–Sulfur Batteries via Molecular Layer Deposited Coating. Nano Letters, 2016, 16, 3545-3549.	9.1	157
9	Investigation of surface effects through the application of the functional binders in lithium sulfur batteries. Nano Energy, 2015, 16, 28-37.	16.0	112
10	Two-Dimensional Mesoporous Carbon Doped with Fe–N Active Sites for Efficient Oxygen Reduction. ACS Catalysis, 2017, 7, 7638-7646.	11.2	90
11	Atomic-Level Construction of Tensile-Strained PdFe Alloy Surface toward Highly Efficient Oxygen Reduction Electrocatalysis. Nano Letters, 2020, 20, 1403-1409.	9.1	89
12	Photocatalytic Color Switching of Transition Metal Hexacyanometalate Nanoparticles for High-Performance Light-Printable Rewritable Paper. Nano Letters, 2017, 17, 755-761.	9.1	83
13	Generalized Synthetic Strategy for Transition-Metal-Doped Brookite-Phase TiO <sub>2</sub> Nanorods. Journal of the American Chemical Society, 2019, 141, 16548-16552.	13.7	78
14	Enhanced Photoreversible Color Switching of Redox Dyes Catalyzed by Bariumâ€Doped TiO <sub>2</sub> Nanocrystals. Angewandte Chemie - International Edition, 2015, 54, 1321-1326.	13.8	70
15	Dramatic differences in carbon dioxide adsorption and initial steps of reduction between silver and copper. Nature Communications, 2019, 10, 1875.	12.8	63
16	<i>In Situ</i> X-ray Absorption Spectroscopic Investigation of the Capacity Degradation Mechanism in Mg/S Batteries. Nano Letters, 2019, 19, 2928-2934.	9.1	63
17	High-performance lithium/sulfur cells with a bi-functionally immobilized sulfur cathode. Nano Energy, 2014, 9, 408-416.	16.0	47
18	Lithium nitrate: A double-edged sword in the rechargeable lithium-sulfur cell. Energy Storage Materials, 2019, 16, 498-504.	18.0	39

YIFAN YE

#	Article	IF	CITATIONS
19	Electrochemical flow cell enabling <i>operando</i> probing of electrocatalyst surfaces by X-ray spectroscopy and diffraction. Physical Chemistry Chemical Physics, 2019, 21, 5402-5408.	2.8	38
20	X-ray Absorption Spectroscopy Characterization of a Li/S Cell. Nanomaterials, 2016, 6, 14.	4.1	32
21	Ca Carboxylate Formation at the Calcium/Poly(methyl methacrylate) Interface. Journal of Physical Chemistry C, 2012, 116, 20465-20471.	3.1	31
22	Unraveling Shuttle Effect and Suppression Strategy in Lithium/Sulfur Cells by In Situ/Operando Xâ€ray Absorption Spectroscopic Characterization. Energy and Environmental Materials, 2021, 4, 222-228.	12.8	31
23	Linking surface chemistry to photovoltage in Sr-substituted LaFeO <sub>3</sub> for water oxidation. Journal of Materials Chemistry A, 2018, 6, 22170-22178.	10.3	27
24	Using soft x-ray absorption spectroscopy to characterize electrode/electrolyte interfaces in-situ and operando. Journal of Electron Spectroscopy and Related Phenomena, 2017, 221, 2-9.	1.7	25
25	Tracking the Local Effect of Fluorine Self-Doping in Anodic TiO <sub>2</sub> Nanotubes. Journal of Physical Chemistry C, 2016, 120, 4623-4628.	3.1	22
26	X-ray spectroscopies studies of the 3d transition metal oxides and applications of photocatalysis. MRS Communications, 2017, 7, 53-66.	1.8	22
27	Revealing <i>In Situ</i> Li Metal Anode Surface Evolution upon Exposure to CO <sub>2</sub> Using Ambient Pressure X-Ray Photoelectron Spectroscopy. ACS Applied Materials & Interfaces, 2020, 12, 26607-26613.	8.0	21
28	Initial Steps in Forming the Electrode–Electrolyte Interface: H2O Adsorption and Complex Formation on the Ag(111) Surface from Combining Quantum Mechanics Calculations and Ambient Pressure X-ray Photoelectron Spectroscopy. Journal of the American Chemical Society, 2019, 141, 6946-6954.	13.7	19
29	Synergy between a Silver–Copper Surface Alloy Composition and Carbon Dioxide Adsorption and Activation. ACS Applied Materials & Interfaces, 2020, 12, 25374-25382.	8.0	19
30	Structural and Optical Interplay of Palladium-Modified TiO <sub>2</sub> Nanoheterostructure. Journal of Physical Chemistry C, 2015, 119, 2222-2230.	3.1	18
31	Strong O 2p–Fe 3d Hybridization Observed in Solution-Grown Hematite Films by Soft X-ray Spectroscopies. Journal of Physical Chemistry B, 2018, 122, 927-932.	2.6	18
32	Electronic structures and chemical reactions at the interface between Li and regioregular poly (3-hexylthiophene). Organic Electronics, 2012, 13, 1060-1067.	2.6	16
33	X-ray-Induced Fragmentation of Imidazolium-Based Ionic Liquids Studied by Soft X-ray Absorption Spectroscopy. Journal of Physical Chemistry Letters, 2018, 9, 785-790.	4.6	14
34	X-ray Absorption Spectroscopic Characterization of the Synthesis Process: Revealing the Interactions in Cetyltrimethylammonium Bromide-Modified Sulfur–Graphene Oxide Nanocomposites. Journal of Physical Chemistry C, 2016, 120, 10111-10117.	3.1	13
35	Predictions of Chemical Shifts for Reactive Intermediates in CO2 Reduction under Operando Conditions. ACS Applied Materials & Interfaces, 2021, 13, 31554-31560.	8.0	12
36	Trace Key Mechanistic Features of the Arsenite Sequestration Reaction with Nanoscale Zerovalent Iron. Journal of the American Chemical Society, 2021, 143, 16538-16548.	13.7	12

YIFAN YE

#	Article	IF	CITATIONS
37	Probing the surface chemistry for reverse water gas shift reaction on Pt(1 1 1) using ambient pressure X-ray photoelectron spectroscopy. Journal of Catalysis, 2020, 391, 123-131.	6.2	11
38	Surface-bound sacrificial electron donors in promoting photocatalytic reduction on titania nanocrystals. Nanoscale, 2019, 11, 19512-19519.	5.6	8
39	In Situ Investigation of the Cu/CH 3 NH 3 PbI 3 Interface in Perovskite Device. Advanced Materials Interfaces, 2021, 8, 2100120.	3.7	8
40	Engineering the metal–organic interface by transferring a high-quality single layer graphene on top of organic materials. Carbon, 2015, 87, 78-86.	10.3	7
41	A facile route for the synthesis of heterogeneous crystal structures in hierarchical architectures with vacancy-driven defects <i>via</i> the oriented attachment growth mechanism. Journal of Materials Chemistry A, 2018, 6, 10663-10673.	10.3	4
42	Low-Temperature Growth Improves Metal/Polymer Interfaces: Vapor-Deposited Ca on PMMA. Journal of Physical Chemistry C, 2014, 118, 6352-6358.	3.1	3
43	Osmotic pressure-induced pocket-like spheres with Fe single-atom sites for the oxygen reduction reaction. Journal of Materials Chemistry A, 2021, 9, 13908-13915.	10.3	3
44	APXPS of Solid/Liquid Interfaces. ACS Symposium Series, 0, , 67-92.	0.5	3
45	An APXPS Probe of Cu/Pd Bimetallic Catalyst Surface Chemistry of CO <sub>2</sub> Toward CO in the Presence of H <sub>2</sub> O and H <sub>2</sub> . Journal of Physical Chemistry C, 2020, 124, 17085-17094.	3.1	2
46	Carbon dioxide adsorption and activation on gallium phosphide surface monitored by ambient pressure x-ray photoelectron spectroscopy. Journal Physics D: Applied Physics, 2021, 54, 234002.	2.8	2